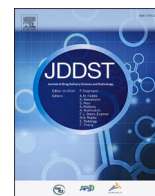




Contents lists available at ScienceDirect

Journal of Drug Delivery Science and Technology

journal homepage: www.elsevier.com/locate/jddst

Research paper

Novel curcumin ascorbic acid cocrystal for improved solubility

Jidnyasa Pantwalawalkar^a, Harinath More^a, Deu Bhangé^b, Udaykumar Patil^a,
Namdeo Jadhav^{a,*}^a Department of Pharmaceutics, Bharati Vidyapeeth College of Pharmacy, Kolhapur, 416013, Maharashtra state, India^b Department of Chemistry, Shivaji University, Kolhapur, 416004, Maharashtra state, India

ARTICLE INFO

Keywords:

Curcumin

Ascorbic acid

In silico screening

Cocrystal

Solubility and dissolution improvement

ABSTRACT

The present investigation aims to develop novel curcumin-ascorbic acid cocrystal for enhancing the solubility, stability, and complementary biological activities for curcumin. Based on *in silico* approach to screen ascorbic acid as a cofomer for curcumin, cocrystals were prepared by the solvent evaporation method, and further evaluated for saturation solubility, cocrystal propensity, physicochemical interactions (FTIR and DSC), XRD, drug dissolution, etc. *In silico* findings confirmed the suitability (H_{ex} , G_{mix}) of ascorbic acid for the cocrystallization of curcumin. The DSC and XRD data of the solvent evaporated curcumin-ascorbic acid mixture confirmed the formation of cocrystal, eutectic, and binary mixture with an excess of cofomer. The binary phase diagram implied 0.5 to the 0.65-mole fraction of curcumin, essential for cocrystallization with ascorbic acid. The novel curcumin ascorbic acid cocrystals revealed extraordinary improvement in aqueous solubility of curcumin, especially, 576 fold in distilled water, 10 fold in the buffer pH 1.2, and 9 fold in the buffer pH 6.8. The curcumin-ascorbic acid cocrystal system exhibited a superior dissolution profile compared to neat curcumin. Thus, ascorbic acid has enunciated its role as a cofomer for curcumin in cocrystal formation, which has been complemented by predicted complementary biological activities, and stability (acidic milieu).

1. Introduction

Curcumin (diferuloylmethane); a polyfunctional phytochemical, has been extensively used as an antioxidant, anti-inflammatory, anticancer, antiulcer, anti-Alzheimer, antibacterial [1,2], etc. Due to a multitude of pharmacological actions, it has been widely investigated physicochemically and physico-technically, to enable efficient and efficacious pharmaceutical formulation design. The vital aspect of formulation design and biological activities is its polymorphic and crystal form and physicochemical properties. Reportedly, it exhibits three polymorphs [3,4]. Amongst them, form 1 (monoclinic) is relatively stable compared to form 2 and form 3. From the dissolution viewpoint, form 2 (orthorhombic) dissolves rapidly, whereas form 3 (orthorhombic) has been reported to be unstable and hence its reproducibility is a key concern [3, 4].

Despite appreciable safety, even at high doses in humans (12 g/day); its therapeutic effectiveness is limited due to poor aqueous solubility and pH-dependent instability [5–7]. Precisely, rapid decomposition at neutral and alkaline pH (>90% in 30 min) is a drawback [6,7]. The problem stems from the hydrophobic polyphenol ring in its structure

[8]. Poor absorption, rapid metabolism, fast systemic elimination, poor bioavailability, are its consequences [8–10].

To improve the solubility and stability of curcumin, numerous novel approaches have been adopted by workers viz: liposomes, nanoparticles, bioemulsion, micelles, films, micro/nanoencapsulation [11–23], etc. Concomitant administration of curcumin with lecithin, quercetin, genistein, eugenol, terpinol has also been attempted [24]. Complexation of curcumin with robusoside and phosphatidylcholine in equimolar quantities has been successfully demonstrated [25]. In furtherance to it, lucrative strategies like the formation of nanofibers, metal complexes, cocrystals, eutectic mixtures, co-amorphous mixtures [26–41], etc. have been tried and seem appreciable. Certainly, aforesaid strategies imply improved solubility, dissolution, and bioavailability to curcumin.

Recently, cocrystallization has been marked as a novel promising approach, to improve the solubility of curcumin. It offers a simple, feasible, and cost-effective method, sometimes green as well. Various cofomers like resorcinol, pyrogallol, isonicotinamide, gallic acid, cinnamic acid, hydroxyquinol, dextrose have reported for cocrystallization of curcumin hitherto [30–35]. Eutectic mixtures running alongside, have been formulated for curcumin using cofomers like salicylic acid,

* Corresponding author.

E-mail address: nrjadhav18@rediffmail.com (N. Jadhav).<https://doi.org/10.1016/j.jddst.2020.102233>

Received 19 August 2020; Received in revised form 12 October 2020; Accepted 15 November 2020

Available online 23 November 2020

1773-2247/© 2020 Elsevier B.V. All rights reserved.

nicotinamide, ferulic acid, hydroquinone, p-hydroxybenzoic acid, L-tartaric acid, succinic acid, paracetamol, carbamazepine, ethylparaben, glycine, tyrosine, N-acetyl D, L-tryptophan, biotin [36,37]. To take the incentive of amorphism, co-amorphization of curcumin has been researched using artemisin, piperazine and folic acid dehydrate as cofomers [38–41]. Collectively, results seem promising for cocrystal/eutectic/co-amorphous systems of curcumin.

Amongst studies reported on curcumin, to date, selection of cofomer in the view of pharmacological relevance and stabilization has been scarcely reported. To reap the benefits of pharmacodynamic relevance, we have demonstrated microenvironmental pH regulation/stabilization of curcumin microspheres using ascorbic acid [42]. Since, ascorbic acid has complementary pharmacological activities (antioxidant, anti-inflammatory, anti-Alzheimer's, anticancer, etc.) to curcumin, pharmacological relevance coupled with stabilization of curcumin in an acidic milieu could outweigh the work reported till date [43–46]. Ascorbic acid, due to the possibility of structural interactions, may enhance solubility and dissolution of curcumin. As ascorbic acid shares structural similarity with curcumin, one of the essential factors required for cocrystallization would be met. Thus, we thought of using ascorbic acid as a cofomer for the generation of curcumin cocrystals. *In silico* approach was employed to screen cofomers for curcumin. The curcumin-ascorbic acid cocrystals were prepared using a solvent evaporation method and evaluated for solubility, physicochemical interactions (FTIR and DSC), XRD, drug dissolution, etc.

2. Materials and methods

2.1. Material

Curcumin was received as a gift sample from Sunpure Extracts, Delhi, India. Ascorbic acid and methanol (analytical grade) were purchased from LobaChemie Pvt. Ltd, Mumbai, Maharashtra, India.

2.2. In silico studies

2.2.1. Suitability of ascorbic acid as a cofomer

To assess the probability of cocrystal formation of curcumin with ascorbic acid; it was primarily screened by COSMOquick software. For validation, reported cofomers of curcumin were also screened (*in silico*) for cocrystallization, using the same software. The input structures were given in SMILE string and the values of H_{ex} , H_{hb} , G_{mix} , f_{fit} , similarity, frag_quality, and cofomer ranking were calculated using the software. Along with the prediction of these parameters, additional information about the rotatable bond, ring bond, conjugated bond, and internal bond was obtained. The data were compared with the output of previously reported curcumin cocrystals. Based on the structure of the curcumin and cofomer (ascorbic acid), fusion temperature, enthalpy, and solubility; the ternary phase diagram was obtained using COSMO-quick software. The ternary phase diagram was used to predict the probable stoichiometric ratios favoring cocrystallization.

2.2.2. Biological activity prediction

PASS Online (Prediction of Activity Spectra for Substances) software was used to predict the pharmacological activities of curcumin and cofomers (ascorbic acid and reported). The structural formula input was given to the software and the values of P_a (probability of compound to be active) and P_i (probability of compound to be inactive) were obtained.

2.2.3. Virtual interactions

V-Life MDS 4.6 software was used to study physicochemical interactions between curcumin and ascorbic acid. Virtual interactions between curcumin and reported cofomers used for cocrystallization i.e. resorcinol, pyrogallol, cinnamic acid, dextrose, gallic acid, and isonicotinamide, were also studied. Initially, 2D structures of all

compounds were drawn on the V-Life Engine and converted to 3D structures. The energy of each molecule was minimized to generate stable structures and further subject to interaction analysis module, to unveil interactions of curcumin with various conformers.

2.2.4. Preparation and evaluation of curcumin cocrystals

2.2.4.1. Construction of binary phase diagram. The stoichiometric ratio for cocrystallization or eutectic mixture formation can be predicted by plotting the binary phase diagram for drug and cofomer. The same can also be investigated by the melting behavior of drugs and cofomer. For cocrystallization, physical mixtures of curcumin and ascorbic acid covering entire composition range i.e. 0.1, 0.2, 0.3, 0.4, 0.5, 0.6, 0.7, 0.8, 0.9 (mole fraction of curcumin) were ground in mortar using pestle for 10 min. Differential Scanning Calorimetry (Lab METTLER) was used to analyze the thermal behavior of curcumin-ascorbic acid physical mixtures. Approximately, 3 mg sample of each physical mixture (each mole fraction) was placed in an aluminum pan and the melting behavior was recorded from ambient temperature to 300 °C with a 10 °C/min heating rate. The flow of nitrogen gas was maintained over the sample to create a reproducible and dry atmosphere and hence to eliminate the possibility of air oxidation of samples at higher temperatures. The onset temperature of the first endothermic peak in the DSC thermogram was considered as a solidus point and the peak temperature (lowest endotherm temperature point) of the second endotherm was considered as liquidus point for phase diagram construction [34].

Further, based on the binary phase diagram, the probable mixtures likely generating cocrystals were prepared by solid-state grinding for 10 min, using mortar and pestle. Subsequently, likely cocrystal mixtures were dissolved in solvent methanol, and further solvent completely removed by Rotary Evaporator (Heidolph, Germany) at 100 RPM and 50 °C [34].

2.3. Saturation solubility

Saturation solubility study for curcumin-ascorbic acid mixtures was performed by phase solubility method, in triplicate. An excess amount (50 mg) of curcumin, ascorbic acid, physical mixtures of curcumin-ascorbic acid, and the solvent evaporated curcumin-ascorbic acid mixture were dissolved separately in a conical flask containing 10 ml of distilled water, buffer (pH 1.2 and pH 6.8). Further, the dispersions were stirred at 37 °C for 72 h in Orbital Shaker. After equilibrium, the samples were centrifuged at 2000 rpm for 15 min. Subsequently, the supernatant was filtered through Whatman filter paper no. 45 and absorbances were measured at λ_{max} 425 nm using a UV visible spectrophotometer (Shimadzu UV-1800 Spectrophotometer, Shimadzu, Japan) [47].

2.4. Differential scanning Calorimetry (DSC)

The DSC thermograms of curcumin, ascorbic acid, physical mixture of curcumin-ascorbic acid (0.1–0.9 mol fraction of curcumin) were recorded. Thermograms of solvent evaporated curcumin-ascorbic acid mixtures (0.50–0.65 mol fraction of curcumin) were also recorded using DSC (Lab METTLER) over the temperature range of ambient to 300 °C with 10 °C/min heating rate.

2.5. X-ray diffraction studies

Powder X-ray diffraction data (XRD) of neat curcumin, ascorbic acid, and cocrystal was obtained on D2 PhaserBruker diffractometer equipped with beta filtered Cu K α ($\lambda = 1.5418 \text{ \AA}$) source of x-rays. The powder diffraction data was collected in a 2θ range 5–50° with a step size of 0.02°. The crystallographic information files of curcumin and ascorbic acid were taken from literature to simulate XRD patterns of the same for the sake of comparison using Mercury (4.1.3 free version) [48,49].

2.6. FTIR spectroscopy

FTIR spectra of neat curcumin, ascorbic acid, and the solvent evaporated curcumin-ascorbic acid mixture were recorded by the FTIR spectrophotometer (Jasco 4700) to observe physicochemical interactions. The samples were scanned between the wavenumber of 4000 to 400 cm^{-1} with a resolution of 2 cm^{-1} .

2.7. In-vitro dissolution study

Curcumin, curcumin-ascorbic acid physical mixture and curcumin-ascorbic acid cocrystal were evaluated for the *in-vitro* dissolution study to compute and compare the improvement in drug dissolution over neat curcumin. A known quantity of samples (neat curcumin or curcumin-ascorbic acid physical mixture or curcumin-ascorbic acid cocrystal equivalent to 20 mg of pure curcumin) were placed in contact with dissolution media i.e. distilled water, buffer pH 1.2, and buffer pH 6.8 (1 L) and incubated in an orbital shaker at 37 ± 0.5 °C and 100 rpm. 1 ml samples were withdrawn at the time interval of 15, 30, 45, 60, 75, 90, 105, and 120 min and replaced with the same volume of fresh medium. Further, all samples were filtered, diluted, and analyzed at λ_{max} 425 nm using a UV visible spectrophotometer (Shimadzu UV- 1800 Spectrophotometer, Shimadzu, Japan). All experiments were performed in triplicate [47,50].

3. Result and discussion

3.1. In silico studies

3.1.1. Suitability of ascorbic acid as a coformer

Computational screening of ascorbic acid as a coformer for the cocrystallization of curcumin was assessed using CosmoQuick Software. Based on structural relevance and interaction propensity between two, the values of H_{hb} (enthalpy due to hydrogen bonding) and H_{ex} (excess enthalpy) obtained were -0.241 and -0.281 respectively. As both H_{hb} and H_{ex} values contribute to the total enthalpy of a system which should be low for the formation of a stable system; the lower H_{hb} and H_{ex} values indicated a high probability of cocrystallization. The G_{mix} value (free energy) was found to be -0.30 . The value of f_{fit} was observed to be 7.878, which depends on excess enthalpy and molecular flexibility of drug and coformer. Both G_{mix} and f_{fit} values divulged cocrystallization because free energy should be low for the formation of a stable system, and f_{fit} value should be optimum for bond formation between drug and coformer. The similarity value 9, means both the compounds have sufficient structural similarity which is necessary for cocrystallization. The value of fragmentation was found to be 0 which favored the prediction of cocrystal. Based on the aforesaid parameters, coformer ranking was given by software as 1, which indicated the cocrystallization suitability of ascorbic acid for curcumin. Alongside parameters; the presence of 6 rotatable bonds, 5 ring bonds, 3 conjugated bonds, and 9 internal bonds in the cocrystal system were also predicted by the software (Table 1). The values of all parameters for test coformer (ascorbic acid) lie in the range of reported, thus corroborates the prediction.

Table 1

In silico cocrystal screening data for curcumin and coformers by COSMOquick software.

Coformer type	Coformer	H_{hb}	H_{ex}	G_{mix}	f_{fit}	Similarity	fragmentation	Coformer ranking	Rotatable bonds	Ring bonds	Conjugated bonds	Internal bonds
Test	Ascorbic Acid	-0.24	-0.28	-0.30	7.87	9.00	0	1	6	5	3	9
Reported	Cinnamic Acid	-0.07	-0.08	-0.37	6.54	5.27	2	1	3	6	9	0
Reported	Gallic Acid	-0.86	-1.21	-0.67	6.43	4.33	3	1	5	6	7	4
Reported	Hydroxyquinol	-1.14	-1.86	-0.87	4.76	4.11	3	1	3	6	6	2
Reported	Isonicotinamide	-0.31	-0.27	-0.34	5.84	9.00	0	1	2	6	8	0
Reported	Resorcinol	-0.82	-1.09	-0.66	5.02	9.00	0	1	2	6	6	0
Reported	Pyrogallol	-0.73	-0.96	-0.63	5.66	4.33	4	1	3	6	6	4

The interpretations of the ternary phase diagram (Fig. 1) could guide about the presence of different phases like the solution phase, the combination of solution and cocrystal phase, a mixture of solution and solute 1 (curcumin), a combination of solutions, cocrystal curcumin, and mixture of the solution, cocrystal and solute 2 (ascorbic acid). This deciphered the formation of a mixture of the cocrystal phase, comprising a solution of curcumin/ascorbic acid, and cocrystal.

3.1.2. Biological activity prediction

The data provided in Table 2 represents the predicted biological activities of curcumin and ascorbic acid. An output of PASS online software demonstrated that both curcumin and ascorbic acid share many common pharmacological activities like antineoplastic, vaso-protector, antioxidant, chemoprotective, antieczematic, cardiovascular analeptic, antiulcerative, antiseborrheic, antiviral, antibacterial, anti-inflammatory, etc. The software output on biological activities of both could entail the effectiveness of duo in the treatment of cancer.

Besides these common pharmacological actions, additional predictions were made for curcumin, through high Pa scores. Prominent predictions were about the treatment of colon cancer, gastric cancer, brain cancer, breast cancer, lung cancer, liver cancer, bone cancer, bladder cancer, etc. Surprisingly, ascorbic acid outputted significant Pa values for antiarthritic, anticataract activities (data not provided).

The software predictions about reported coformers were in agreement with the uses of cinnamic acid as antimutagenic, antihypoxic, antiseborrheic, and antieczematic. Dextrose as sweetener, vaso-protective, antitoxic, antineoplastic, immunostimulant, radioprotective, and Gallic acid, hydroxyquinol, isonicotinamide as antiseptic, peroxidase inhibitor, fibrinolytic, antiseborrheic, and astringent. The software predicted the effectiveness of resorcinol and pyrogallol in alopecia treatment (Table 3). Thus, the Pa values given by software for reported coformers validated the findings for curcumin and ascorbic acid. The value of $P_a > P_i$ could be a threshold value for significant predicted activities.

3.1.3. Virtual interactions

Ascorbic acid showed van der Waal and hydrophobic interactions with curcumin. Dextrose showed similar interactions with curcumin and additional hydrogen bonding. Isonicotinamide, pyrogallol, and resorcinol showed aromatic interaction along with van der Waal interaction, with curcumin. Cinnamic acid-curcumin showed van der Waal interactions with the absence of both aromatic and hydrophobic interactions (Table 4, Fig. 2). The net interaction score of curcumin ascorbic acid (34) could lie in the range (22–51) of reported ones thus might have the propensity to form cocrystal.

3.1.4. Preparation of curcumin cocrystal: Construction of binary phase diagram

The DSC thermograms of Curcumin-Ascorbic acid physical mixture covering the entire composition range have been depicted in Fig. 3. As anticipated, W shaped curve was observed in the binary phase diagram (solidus and liquidus points) indicating the possibility of cocrystal formation (Fig. 4). The mole fraction of curcumin (0.5–0.65) was assumed to be a region of cocrystallization. Thus, 0.50, 0.55, 0.60, and 0.65-mole

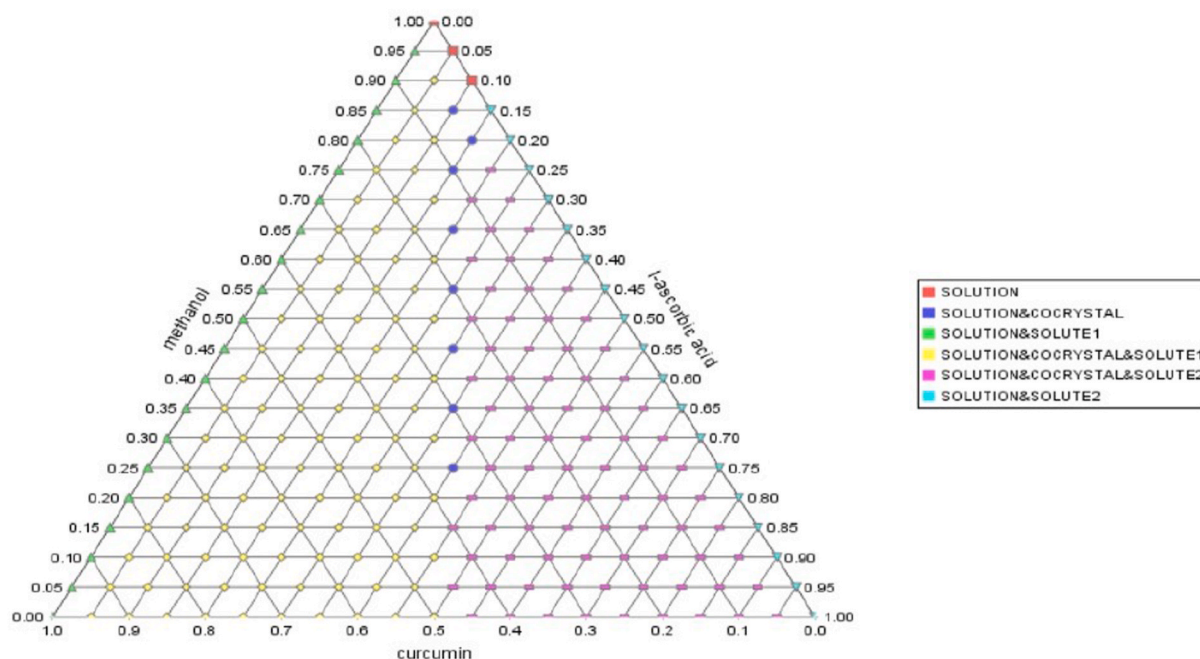


Fig. 1. Ternary phase diagram for Curcumin-Ascorbic acid-Methanol system.

Table 2

Biological activity prediction data for curcumin and ascorbic acid, obtained by PASS Online software^a.

Curcumin		Ascorbic acid			
Activity	Pa	Pi	Activity	Pa	Pi
Reductant	0.864	0.003	Reductant	0.864	0.003
Vasoprotector	0.678	0.012	Vasoprotector	0.948	0.002
Anti-inflammatory	0.677	0.019	Anti-inflammatory	0.779	0.008
Antineoplastic	0.672	0.031	Antineoplastic	0.617	0.041
Antitumor	0.651	0.007	Antitumor	0.522	0.019
Oxygen scavenger	0.650	0.013	Oxygen scavenger	0.889	0.001
Antiseborrheic	0.624	0.051	Antiseborrheic	0.542	0.065
Antieczematous	0.623	0.076	Antieczematous	0.682	0.052
Antioxidant	0.610	0.004	Antioxidant	0.928	0.003
Antimycobacterial	0.608	0.009	Antibacterial	0.377	0.036
CVS analeptic	0.535	0.020	CVS analeptic	0.564	0.018
Antiviral	0.418	0.013	Antiviral	0.567	0.009
Antineoplastic (non-Hodgkin's lymphoma)	0.387	0.120	Antineoplastic (non-Hodgkin's lymphoma)	0.393	0.114
Thyroid Cancer	0.160	0.100	Thyroid cancer	0.168	0.078

^a indicates overlapping activities in curcumin and ascorbic acid.

fractions of curcumin were selected for the cocrystallization zone based on the binary phase diagram.

3.2. Evaluation of cocrystals

3.2.1. Saturation solubility

Saturation solubility of neat curcumin was found to be 0.002 ± 0.0002 mg/ml in water, 0.041 ± 0.0032 mg/ml in buffer pH 1.2, and 0.127 ± 0.0095 mg/ml in buffer pH 6.8. Ascorbic acid had a saturation solubility 3.1 ± 0.1241 mg/ml in water, 0.263 ± 0.0132 mg/ml in buffer pH 1.2, and 0.31 ± 0.0139 mg/ml in buffer pH 6.8. The curcumin-ascorbic acid physical mixtures showed improved solubility compared to neat curcumin. Amongst the curcumin-ascorbic acid mixtures, the 0.5-mole fraction of curcumin showed the highest saturation solubility i. e. 0.908 ± 0.0545 mg/ml in water, 0.264 ± 0.0238 mg/ml at pH buffer 1.2, and 1.146 ± 0.0459 mg/ml at buffer pH 6.8. An increase in the solubility of physical mixtures could be attributed to polymorphic

Table 3

Predicted biological activity of reported cofomers used for cocrystallization of curcumin.

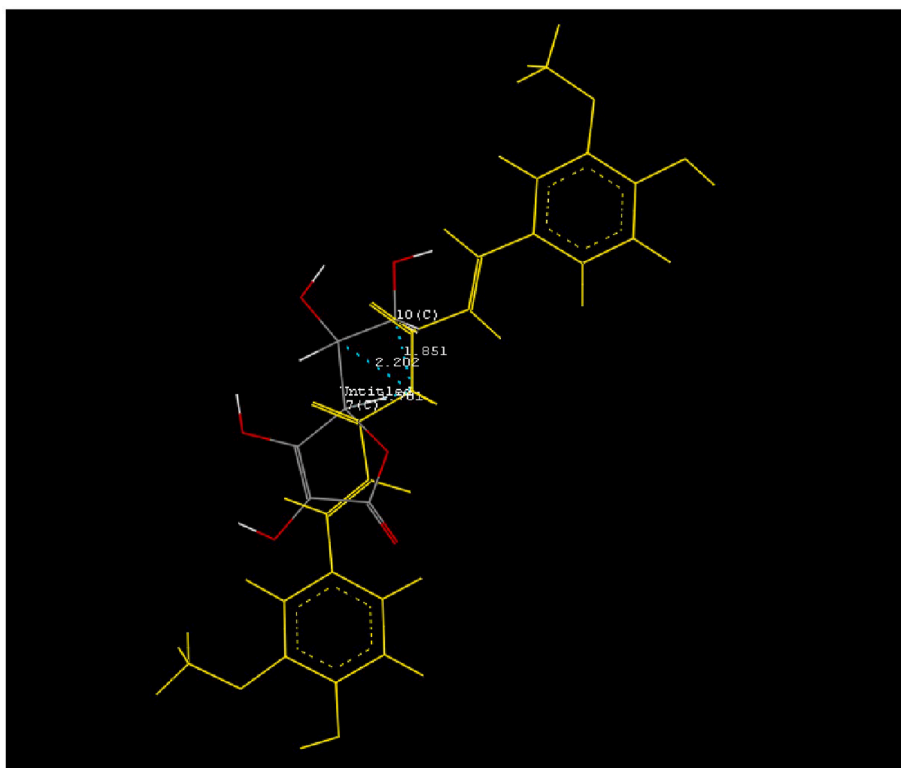
Cinnamic acid		Gallic acid			
Activity	Pa	Pi	Activity	Pa	Pi
Antimutagenic	0.817	0.004	Antiseptic	0.910	0.003
Antihypoxic	0.814	0.004	Peroxidase inhibitor	0.891	0.003
Antiseborrheic	0.805	0.018	Antieczematous	0.855	0.009
Carminative	0.778	0.004	Antiseborrheic	0.835	0.013
Antieczematous	0.772	0.025	Antifungal	0.828	0.005
Vasoprotector	0.748	0.008	Fibrinolytic	0.823	0.004
Oxygen scavenger	0.720	0.005	Astringent	0.812	0.001
Antipsoriatic	0.692	0.005	Hydroxyquinol		
Dextrose			Antiseborrheic	0.926	0.003
Sweetener	0.890	0.001	Peroxidase inhibitor	0.909	0.003
Vasoprotector	0.887	0.003	Cardiovascular	0.864	0.004
Anti-infective	0.871	0.004	analeptic		
Antitoxic	0.867	0.002	Antimutagenic	0.803	0.004
Antineoplastic	0.833	0.008	Vasoprotector	0.793	0.005
Respiratory	0.822	0.007	Carminative	0.788	0.004
analeptic			Antiseptic	0.773	0.004
Immunostimulant	0.812	0.008	Fibrinolytic	0.771	0.006
Antihypoxic	0.805	0.004	Astringent	0.749	0.002
Antidiabetic	0.781	0.005	Antidyskinetic	0.718	0.014
Antioxidant	0.778	0.004	Reluctant	0.714	0.005
Radioprotector	0.773	0.006	Antihypoxic	0.698	0.008
Analeptic	0.757	0.007	Isonicotinamide		
Laxative	0.752	0.002	Antiseborrheic	0.751	0.028
Anti-inflammatory	0.702	0.015	Peroxidase inhibitor	0.727	0.009
Antiviral	0.697	0.005	oxygen scavenger	0.708	0.005
(Influenza)					
Anthelmintic	0.660	0.005	Fibrinolytic	0.688	0.027
Resorcinol			Antimutagenic	0.771	0.009
CVS analeptic	0.814	0.004	Antiviral	0.649	0.011
			(Picornavirus)		
Alopecia treatment	0.790	0.003	Pyrogallol		
Vasoprotector	0.772	0.006	Peroxidase inhibitor	0.900	0.003
Antimutagenic	0.767	0.004	Antiseborrheic	0.897	0.004
Fibrinolytic	0.765	0.007	CVS analeptic	0.818	0.004
Antiseptic	0.709	0.005	Carminative	0.788	0.004
Oxygen scavenger	0.704	0.006	Alopecia treatment	0.753	0.004

Table 4

Virtual interaction data for curcumin and cofomers.

Cofomers	Interactions and score				Net Interaction score
	Hydrogen Bond	VDW	Hydrophobic Interactions	Aromatic Interactions	
Ascorbic acid	NA	31	3	NA	34
Cinnamic acid	NA	47	NA	NA	47
Dextrose	1	45	5	NA	51
Gallic acid	NA	27	NA	NA	27
Isonicotinamide	NA	21	NA	1	22
Resorcinol	NA	32	NA	1	33
Pyrogallol	NA	40	NA	1	41

NA- Not Observed; VDW- Van der Waal.

**Fig. 2.** Data for virtual interactions between Curcumin and Ascorbic acid.

transformation. It was observed that some amount of polymorphic form 1 was transformed to polymorphic form 2 during solid-state grinding which was absent in neat curcumin. As polymorphic form 2 exhibits comparatively higher solubility; the physical mixture showed enhanced solubility of curcumin. However, as polymorphic form 2 is comparatively less stable than polymorphic form 1; it gets reverted to polymorphic form 1 which reduces solubility with time. The solubility of the solvent evaporated curcumin ascorbic acid mixture (cocrystal) was found to be 1.153 ± 0.0692 mg/ml in water, 0.422 ± 0.0101 mg/ml in buffer at pH 1.2, and 1.241 ± 0.0869 mg/ml in buffer pH 6.8 (Fig. 5). Increased solubility of curcumin in the cocrystal system could be attributed to stronger molecular level interactions between curcumin and ascorbic acid favored by solvent (methanol). As solubility improvement in the cocrystal system was independent of polymorphic transformation (neat curcumin and cocrystal showed the presence of polymorphic form 1); it can consistently exhibit better solubility profile compared to the physical mixture. Saturation solubility of solvent evaporated curcumin ascorbic acid mixture was found to be significantly higher ($P < 0.05$), compared to neat curcumin and physical mixtures.

3.2.2. Differential scanning calorimetry

The DSC thermogram of curcumin having mole fractions ranging from 0.3 to 0.5, could demonstrate two endothermic transitions. At 0.3 mole fraction of curcumin, the first endothermic peak (onset-160.72 °C and peak-188.87 °C) represented the melting of the eutectic mixture followed by the second endothermic peak representing cocrystal melting. Similar thermograms were observed in the case of curcumin mole fractions 0.40 (onset-161.36 °C peak-189.13 °C) and 0.50 (onset-158.55 °C peak-186.49 °C), demonstrating the first endothermic peak corresponding to eutectic melting and second endothermic peak corresponding to melting of cocrystal.

As shown in Fig. 6; the DSC thermogram of the 0.60-mole fraction of curcumin showed the presence of three endothermic peaks, out of which the first endothermic peak represented the melting temperature of eutectic mixture (onset- 158.58 °C and peak- 166.47 °C), second endothermic peak corresponded to melting temperature of cocrystal with an excess of cofomer to form supersaturated liquid melt recrystallized to form cocrystal (onset-173.19 °C and peak- 175.75 °C). The melting of cocrystal has been denoted by the presence of a third endothermic peak having onset at 183.03 °C and peak at 187.10 °C. A similar thermogram was observed in the case of a 0.65-mole fraction of curcumin. Out of

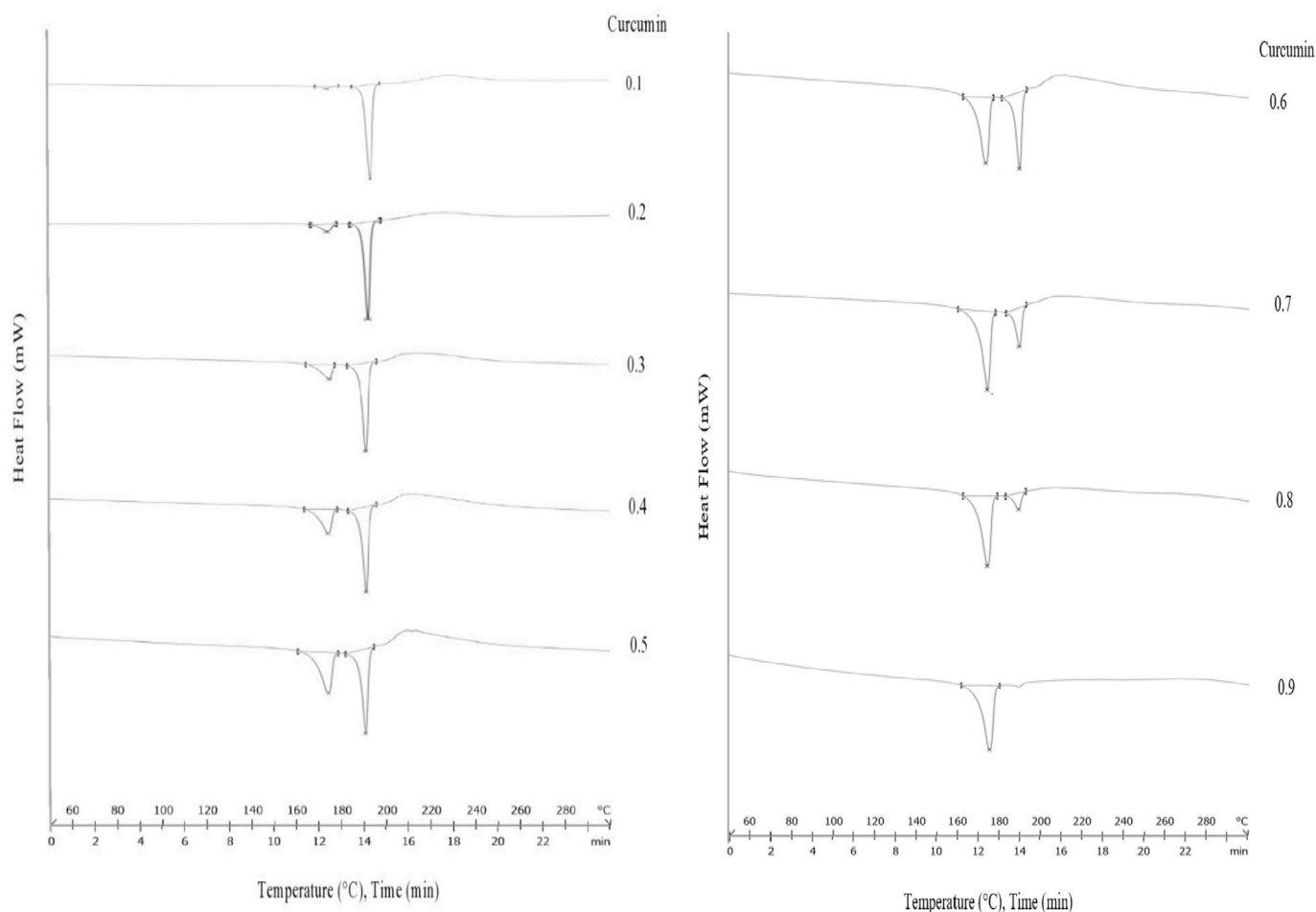


Fig. 3. DSC thermogram of Curcumin and Ascorbic acid physical mixture (0.1–0.9 mol fractions of curcumin).

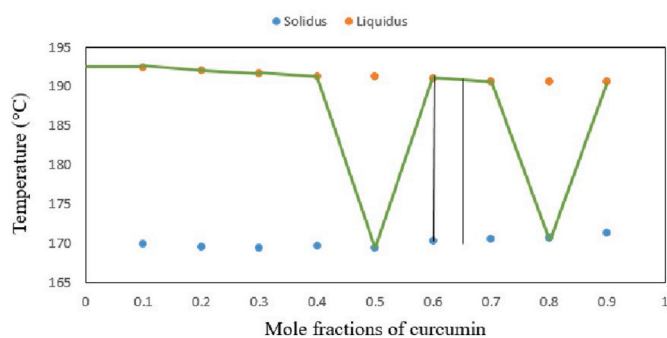


Fig. 4. Binary phase diagram for Curcumin-Ascorbic acid system showing solidus and liquidus temperatures.

three endothermic peaks, a first endothermic peak was observed at an onset temperature of 158.38 °C and a peak temperature of 166.80 °C, followed by a second endothermic peak (onset- 173 °C and peak 173.41), and the third endothermic peak (onset- 185.73 °C and peak-188.82 °C). The corresponding endothermic transitions correspond to eutectic melting, melting of cocrystal with an excess of coformer, and melting of cocrystal respectively.

3.3. X-ray diffraction studies

XRD is a powerful tool to study the crystal structures of crystalline pharmaceutical materials. Some of the pharmaceutical materials bear

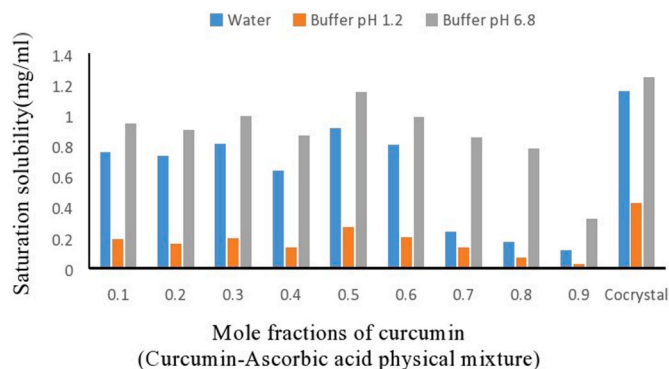


Fig. 5. Saturation solubility of Curcumin-Ascorbic acid physical mixtures and cocrystal.

different crystal structures (crystallographic phases) based on the synthesis/crystallization conditions. These crystallographic phases retain the same molecular formula but have a different arrangement of these molecules in three dimensions, thereby having different physical properties. These different crystal structures can be distinguished from each other by XRD data. Each material has a characteristic XRD pattern thus making this tool a fingerprint technique to identify the appropriate phase of the same. In this viewpoint, we have characterized the precursors' curcumin and ascorbic acid using the powder XRD technique. Powder XRD data collected for the curcumin sample is displayed in Fig. 7 along with the overlay of the simulated (theoretically calculated)

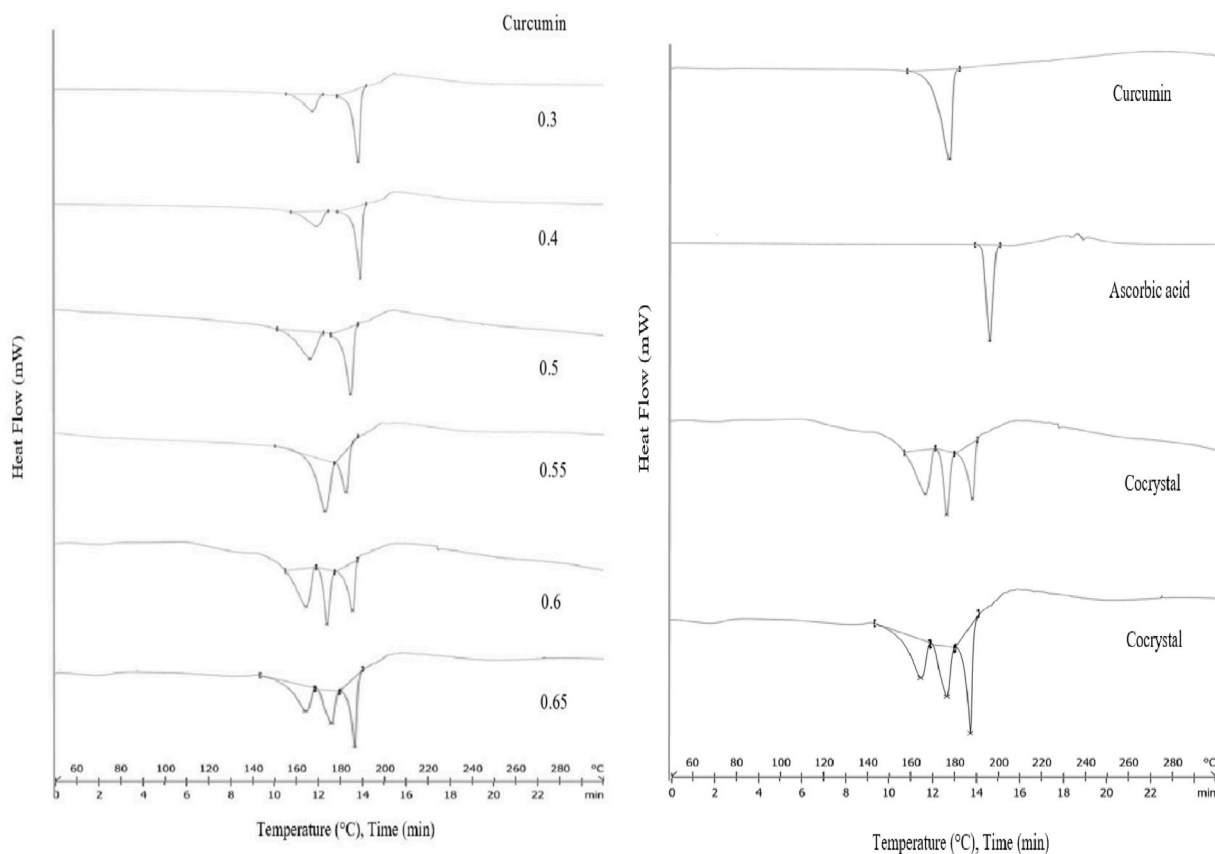


Fig. 6. DSC thermogram of solvent evaporated Curcumin-Ascorbic acid cocrystals (0.3–0.65 mol fractions of curcumin).

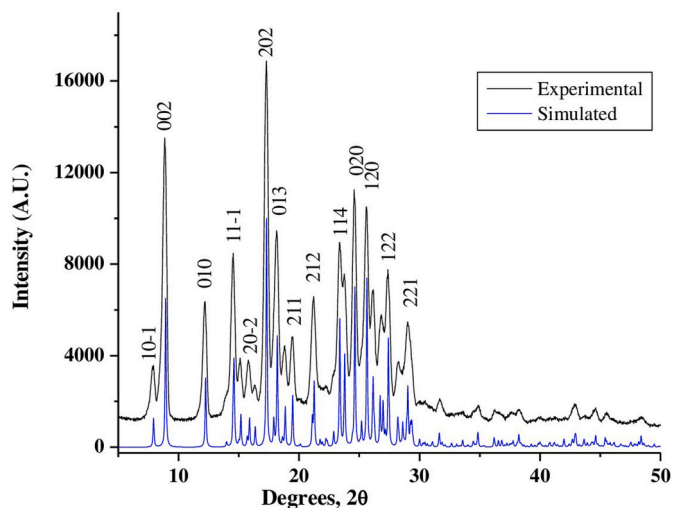


Fig. 7. Powder X-ray diffraction pattern of curcumin (black line) and the simulated pattern of curcumin (blue line). (For interpretation of the references to colour in this figure legend, the reader is referred to the Web version of this article.)

XRD pattern of curcumin using the crystallographic data reported in the literature [48,49]. All the peaks in the XRD pattern of curcumin are well indexed to the monoclinic crystal structure reported earlier. The appearance of sharp peaks in the XRD pattern confirms the polycrystalline nature of curcumin. Further, the absence of any un-indexed reflection in the XRD pattern of curcumin indicates its high phase purity. The monoclinic crystal structure of curcumin is based on the four

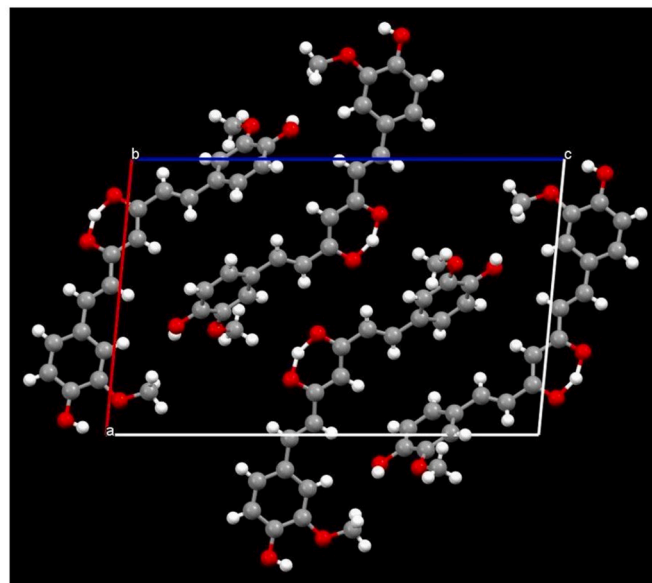


Fig. 8. Ball and stick model of curcumin viewed along 'b' axis (gray-carbon, white-hydrogen, and red-oxygen). (For interpretation of the references to colour in this figure legend, the reader is referred to the Web version of this article.)

molecules in the unit cell and its view along the 'b' axis as displayed in Fig. 8. The XRD pattern of ascorbic acid is similarly plotted in Fig. 9, and its phase purity is also confirmed by indexing all prominent reflections to relevant hkl's shown by its monoclinic crystallographic form. The only mismatch of the intensity of the 002 reflection of ascorbic acid is

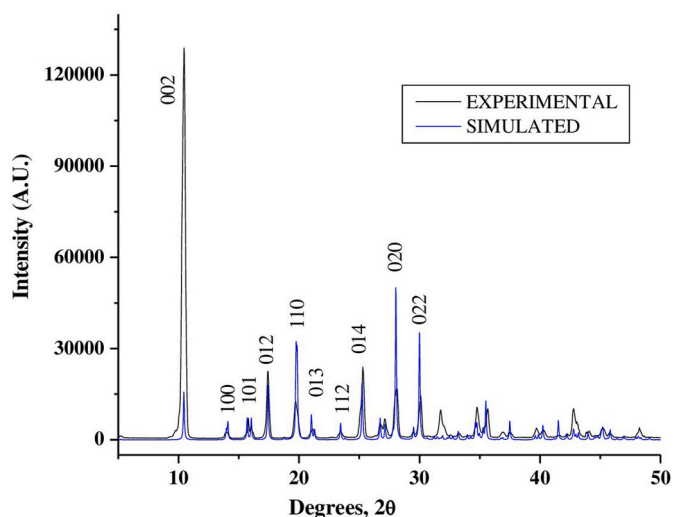


Fig. 9. Powder X-ray diffraction pattern of ascorbic acid (black line) and the simulated pattern of ascorbic acid (blue line). (For interpretation of the references to colour in this figure legend, the reader is referred to the Web version of this article.)

observed and can be ascribed to the preferred orientation of the particles during data collection. This preferred orientation can be removed by rotating the sample during data collection and as such have no impact on the purity of the sample. After confirming the purity of precursors the cocrystals of curcumin and ascorbic acid were allowed to grow as per the protocol described elsewhere in the manuscript.

The XRD pattern of the cocrystal overlapped with those of the precursors is shown in Fig. 10. It is clear from Fig. 10 that the characteristic peaks of the precursor materials are disappeared and new reflections are observed in the XRD pattern of the cocrystal sample. Any phase change of the precursor materials is ruled out by comparing the XRD pattern with available literature XRD patterns of the precursors. The new reflections observed in the cocrystal pattern can be ascribed to the formation of a new phase of a cocrystal formed by an association of ascorbic acid and curcumin. The present data is insufficient to index the crystal system of the cocrystal formed. The interpretation of the powder XRD data is a challenging task as it has severe overlapping of reflections.

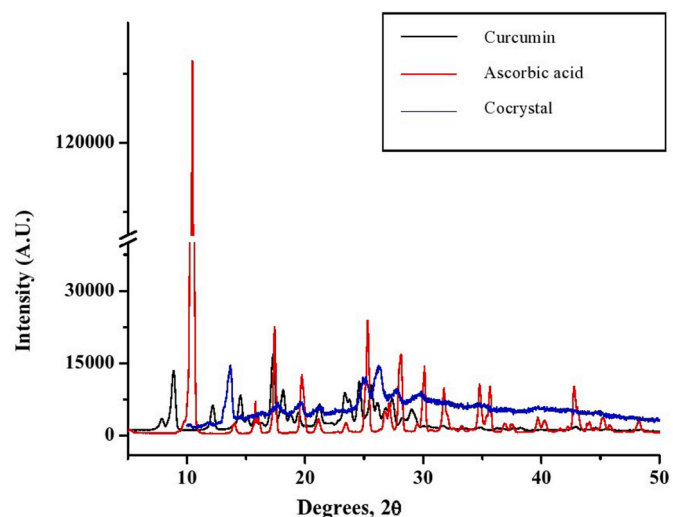


Fig. 10. Powder X-ray diffraction pattern of curcumin (black line), ascorbic acid (red line), and cocrystal (blue line). (For interpretation of the references to colour in this figure legend, the reader is referred to the Web version of this article.)

Although this is the case, the appearance of new reflections and total disappearance of XRD peaks due to precursors used indicates the successful formation of co-crystal of curcumin and ascorbic acid. The characteristic feature in the background of the XRD pattern of cocrystal also indicates the existence of the amorphous content or ill ordered crystallization of the cocrystal. Therefore from the XRD data, it can be concluded that the cocrystallization of curcumin is observed with ascorbic acid and can be further substantiated by the DSC data.

3.4. FTIR spectroscopy

The FTIR is a routine tool used for the analysis of physicochemical interactions amongst pharmaceuticals. We could observe the spectrum of neat curcumin, with a characteristic peak at 3495.62 cm^{-1} representing phenolic O–H stretching. The peaks observed at 1687.19 , 1426.76 , and 1272.54 cm^{-1} represented C=C symmetric aromatic ring stretching vibration, C–H bending vibration, and presence of enol group respectively. In the case of ascorbic acid, characteristic peaks were observed at 3517.39 cm^{-1} , 1745.01 cm^{-1} , and 1642.61 cm^{-1} representing O–H stretching vibration, presence of ester group, and C=O stretching vibration respectively. The FTIR of solvent evaporated curcumin-ascorbic acid mixture showed a different pattern compared to neat curcumin and ascorbic acid. A slight shift of peak to lower wavenumber was noticed. Characteristic peaks at 3495.62 cm^{-1} , 1687.19 cm^{-1} , 1426.76 cm^{-1} and 1272.54 cm^{-1} in FTIR of curcumin were shifted to 3211.60 cm^{-1} , 1684.15 cm^{-1} , 1367.63 cm^{-1} and 1270.56 cm^{-1} respectively. Characteristic peaks at 1745.01 cm^{-1} and 1642.61 cm^{-1} in ascorbic acid were shifted to 1744.52 cm^{-1} and 1633.42 cm^{-1} respectively. This suggested hydrogen bond formation between phenolic OH of curcumin and acidic hydrogen of ascorbic acid (Fig. 11).

3.5. In-vitro dissolution study

The *in-vitro* dissolution profile of curcumin, curcumin-ascorbic acid physical mixture, and curcumin-ascorbic acid cocrystal is depicted in Fig. 12. The *in-vitro* dissolution study demonstrated that $4.216 \pm 0.210\%$, $15.239 \pm 0.685\%$, and $34.121 \pm 1.63\%$ curcumin was dissolved from the sample of neat curcumin in distilled water, buffer pH 1.2 and buffer pH 6.8 respectively at the end of 2 h. Drug dissolution from the physical mixture was found to be $73.931 \pm 2.957\%$, $69.583 \pm 2.623\%$ and $79.052 \pm 3.241\%$ in distilled water, buffer pH 1.2 and buffer pH 6.8 respectively, whereas, the curcumin-ascorbic acid cocrystal system showed $89.214 \pm 3.479\%$, $84.342 \pm 3.153\%$ and $92.361 \pm 3.602\%$ dissolution in distilled water, buffer pH 1.2 and buffer pH 6.8 respectively. This revealed that the curcumin-ascorbic acid cocrystal system exhibited enhanced dissolution compared to pure curcumin and curcumin-ascorbic acid physical mixture which clearly portrays enhanced dissolution of the cocrystal system.

4. Conclusion

The structural suitability and propensity of ascorbic acid towards the cocrystallization of curcumin was confirmed by COSMOquick software. Likely interactions between curcumin and cofomer (ascorbic acid) were elucidated by V. life MDS 4.6 software. Based on the screening by PASS online; it was surfaced that ascorbic acid would help to augment the therapeutic effectiveness of curcumin. The thermal and diffractometric data of solvent evaporated curcumin-ascorbic acid confirmed cocrystal formation, along with eutectic, and excess of cofomer mixtures. The FTIR spectra of solvent evaporated curcumin-ascorbic acid mixture also confirmed hydrogen interactions enabling cocrystal formation. The solubility of curcumin was found to be significantly enhanced ($p < 0.05$) by 576 fold in water, 10 fold in the buffer of pH 1.2, and 9 fold in the buffer of pH 6.8 in curcumin-ascorbic acid cocrystal form Also, superior curcumin dissolution profile was evident from curcumin-ascorbic acid cocrystal system over neat curcumin and curcumin-ascorbic acid

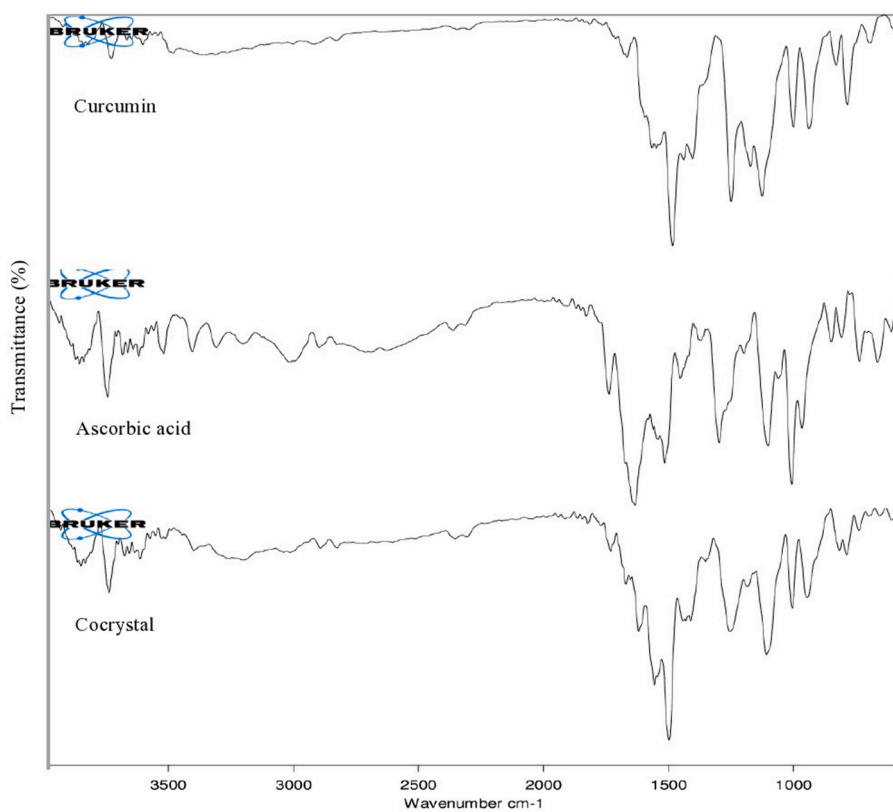


Fig. 11. FTIR spectra for Curcumin, Ascorbic acid, and Cocrystals.

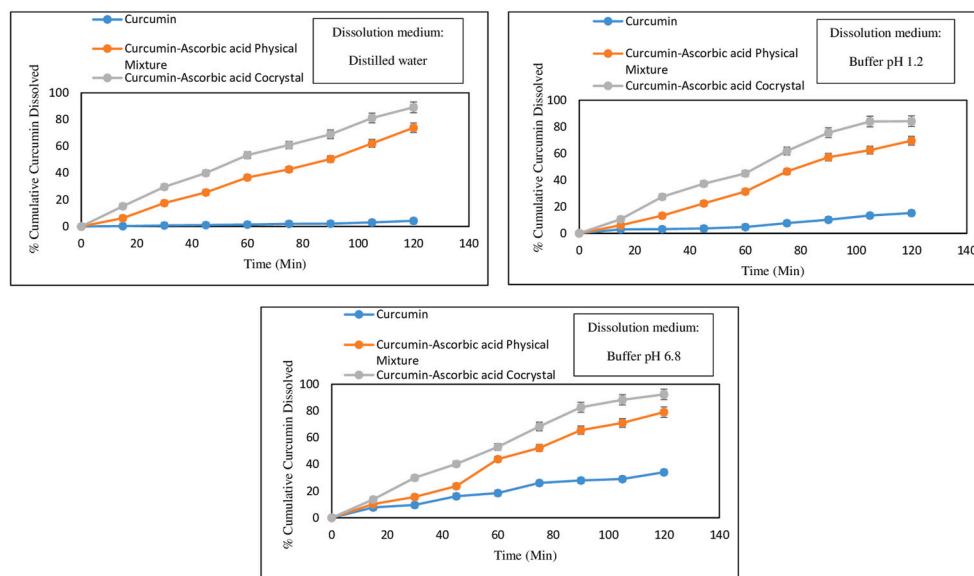


Fig. 12. *In-vitro* dissolution profile of neat Curcumin, Curcumin-Ascorbic acid physical mixture, and Curcumin-Ascorbic acid cocrystal in distilled water, buffer pH 1.2, and buffer pH 6.8.

physical mixture, enunciating the importance of ascorbic acid as a novel cofomer. The stability of curcumin (acidic milieu) and pharmacological complementariness with ascorbic acid has paved the way for speculations about scale-up and pharmacotherapeutic potential.

Declaration of interest

The authors declare no potential conflict of interest.

Funding details

One of the authors is thankful to AICTE, New Delhi for providing financial assistance in the form of the junior research fellowship.

CRediT authorship contribution statement

Jidnyasa Pantwalawalkar: Data curation, Methodology, Writing -

original draft. **Harinath More:** Investigation, Supervision. **Deu Bhang:** Software, Validation, XRD interpretation. **Udaykumar Patil:** Formal analysis, Project administration. **Namdeo Jadhav:** Conceptualization, Supervision, Writing - review & editing.

Acknowledgment

The authors acknowledge Bharati Vidyapeeth College of Pharmacy, Kolhapur (India) for providing research facilities.

References

- [1] K. Vasavda, P.L. Hedge, A. Harini, Pharmacological activities of turmeric (*Curcuma longa* Linn): a review, *J. Homeop. Ayurv. Med.* 2 (2013) 1–4, <https://doi.org/10.4172/2167-1206.1000133>.
- [2] A.R. Mullaicharam, A. Maheswaran, Pharmacological effects of curcumin, *Int. J. Nutr. Pharmacol. Neurol. Dis.* 2 (2012) 92–99, <https://doi.org/10.4103/2231-0738.95930>.
- [3] P. Sanphui, N.R. Goud, U.B. Khandavilli, S. Bhanoth, A. Nangia, New polymorphs of curcumin, *Chem. Commun* 47 (2011) 5013–5015, <https://doi.org/10.1039/c1cc10204d>.
- [4] A.A. Thorat, S.V. Dalvi, Solid-state phase transformations and storage stability of curcumin polymorphs, *Cryst. Growth Des.* 15 (2015) 1757–1770, <https://doi.org/10.1021/cg501814q>.
- [5] S. Qureshi, A.H. Shah, A.M. Ageel, Toxicity studies on *Alpinagalanga* and *Curcuma longa*, *Planta Med.* 58 (1992) 124–127.
- [6] M.K. Modasiya, V.M. Patel, Studies on solubility of curcumin, *Int. J. Pharm. Life Sci.* 3 (2012) 1490–1497.
- [7] Y.-J. Wang, M.-H. Pan, A.-L. Cheng, L.-I. Lin, Y.-S. Ho, C.-Y. Hsieh, J.-K. Lin, Stability of curcumin in buffer solutions and characterization of its degradation products, *J. Pharm. Biomed. Anal.* 15 (1997) 1867–1876, [https://doi.org/10.1016/S0731-7085\(96\)02024-9](https://doi.org/10.1016/S0731-7085(96)02024-9).
- [8] H. Hatcher, R. Planalp, J. Cho, F.M. Torti, S.V. Torti, Curcumin: from ancient medicine to current clinical trials, *Cell. Mol. Life Sci.* 65 (2008) 1631–1652, <https://doi.org/10.1007/s00018-008-7452-4>.
- [9] T. Farooqui, A.A. Farooqui, Curcumin: Historical Background, Chemistry, Pharmacological Action, and Potential Therapeutic Value, *Curcumin for Neurol. Psychiatric Disorders* (2019) 23–44, <https://doi.org/10.1016/B978-0-12-815461-8.00002-5>.
- [10] P. Anand, A.B. Kunnumakkara, R.A. Newman, B.B. Aggarwal, Bioavailability of curcumin: problems and promises, *Mol. Pharm.* 4 (2007) 807–818, <https://doi.org/10.1021/mp700113r>.
- [11] C. Chen, T.D. Johnston, H. Jeon, R. Gedaly, P.P. McHugh, T.G. Burke, D. Ranjan, An in vitro study of liposomal curcumin: stability, toxicity and biological activity in human lymphocytes and Epstein-Barr virus-transformed human B-cells, *Int. J. Pharm.* 366 (2009) 133–139, <https://doi.org/10.1016/j.ijpharm.2008.09.009>.
- [12] J.P. Quinones, H. Peniche, C. Peniche, Chitosan based self-assembled nanoparticles in drug delivery, *Polymers* 10 (2018) 1–32, <https://doi.org/10.3390/polym10030235>.
- [13] L. Mazzzrino, C.L. Dora, I.C. Belletini, E. Minatti, S.G. Cardoso, E. Lemos-Senna, Curcumin-loaded polymeric and lipid nanocapsules: preparation, characterization and chemical stability evaluation, *Lat. Am. J. Pharm.* 29 (2010) 933–940.
- [14] K. Pan, Q. Zhong, S.J. Baek, Enhanced dispersibility and bioactivity of curcumin by encapsulation in casein nanocapsules, *J. Agric. Food Chem.* 61 (2013) 6036–6043, <https://doi.org/10.1021/jf400752a>.
- [15] S.J. Nadaf, S.G. Killedar, Curcuminnanocochleates: use of design of experiments, solid state characterization, in vitro apoptosis and cytotoxicity against breast cancer MCF-7 cells, *J. Drug. Deliv. Sci. Tec* 37 (2018) 337–350, <https://doi.org/10.1016/j.jddst.2018.06.026>.
- [16] S. Alippilakkotte, L. Sreejith, Pectin mediated synthesis of curcumin loaded poly (lactic acid) nanocapsules for cancer treatment, *J. Drug. Deliv. Sci. Tec* 48 (2018) 66–74, <https://doi.org/10.1016/j.jddst.2018.09.001>.
- [17] D. Gaikwad, R. Shewale, V. Patil, D. Mali, U. Gaikwad, N. Jadhav, Enhancement in in vitro anti-angiogenesis activity and cytotoxicity in lung cancer cell by pectin-PVP based curcumin particulates, *Int. J. Bio. Macromol* 104 (2017) 656–664, <https://doi.org/10.1016/j.ijbiomac.2017.05.170>.
- [18] P. Malik, R.K. Ameta, M. Singh, Preparation and characterization of bioemulsions for improving and modulating the antioxidant efficacy of natural phenolic antioxidant curcumin, *Chem. Biol. Interact.* 222 (2014) 77–86, <https://doi.org/10.1016/j.cbi.2014.07.013>.
- [19] S. Patil, B. Choudhary, A. Rathore, K. Roy, K. Mahadik, Enhanced oral bioavailability and anticancer activity of novel curcumin loaded mixed micelles in human lung cancer cells, *Phytomedicine* 22 (2015) 1103–1111, <https://doi.org/10.1016/j.phymed.2015.08.006>.
- [20] E. Portes, C. Gardrat, A. Castellán, V. Coma, Environmentally friendly films based on chitosan and tetrahydrocurcuminoid derivatives exhibiting antibacterial and antioxidative properties, *Carbohydr. Polym* 76 (2009) 578–584, <https://doi.org/10.1016/j.carbpol.2008.11.031>.
- [21] N. Suwannateep, S. Wanichwecharungruang, S.F. Haag, S. Devahastin, N. Groth, J. W. Fluhr, J. Lademann, M.C. Meinke, Encapsulated curcumin results in prolonged curcumin activity in vitro and radical scavenging activity ex vivo on skin after UVB-irradiation, *Eur. J. Pharm. Biopharm.* 82 (2012) 485–490, <https://doi.org/10.1016/j.ejpb.2012.08.010>.
- [22] S.B. de Souza Ferreira, M.L. Bruschi, Improving the bioavailability of curcumin: is micro/nanocapsulation the key? *Ther. Deliv.* 10 (2019) 83–86, <https://doi.org/10.4155/tde-2018-0075>.
- [23] J.O. Akolade, H.O.B. Oloyede, M.O. Salawu, A.O. Amuzat, A.I. Ganiyu, P. C. Onyenekwe, Influence of formulation parameters on encapsulation and release characteristics of curcumin loaded in chitosan-based drug delivery carriers, *J. Drug Deliv. Sci. Technol.* 45 (2018) 11–19, <https://doi.org/10.1016/j.jddst.2018.02.001>.
- [24] P. Anand, Aj.B. Kunnumakkara, R.A. Newman, B.B. Aggarwal, Bioavailability of curcumin: problems and promises, *Mol. Pharm.* 4 (2007) 807–818, <https://doi.org/10.1021/mp700113r>.
- [25] F. Zhang, G.Y. Koh, D.P. Jeanson, J. Hollingsworth, P.S. Russo, G. Vicente, R. W. Stout, Z. Liu, A novel solubility-enhanced curcumin formulation showing stability and maintenance of anticancer activity, *J. Pharm. Sci.* 100 (2011) 2778–2789, <https://doi.org/10.1002/jps.22512>.
- [26] G. Mutlu, S. Calamak, K. Ulubayram, E. Guven, Curcumin-loaded electrospun PHBV nanofibers as potential wound-dressing material, *J. Drug Deliv. Sci. Technol.* 43 (2017) 185–193, <https://doi.org/10.1016/j.jddst.2017.09.017>.
- [27] P.-Z. Li, Z.-Q. Liu, Ferrocenyl-substituted curcumin: can it influence antioxidant activity to protect DNA, *Eur. J. Med. Chem.* 46 (2011) 1821–1826, <https://doi.org/10.1016/j.ejmech.2011.02.041>.
- [28] N. Bicer, E. Yildiz, A.A. Yegani, F. Aksu, Synthesis of curcumin complexes with iron (iii) and manganese (ii) and curcumin-iron (iii) effects on alzheimer's disease, *New J. Chem* 42 (2018) 8098–8104, <https://doi.org/10.1039/c7nj04223j>.
- [29] M.H.M. Leung, T. Harada, T.W. Kee, Delivery of curcumin and medicinal effects of the copper(II)-curcumin complexes, *Curr. Pharm. Des* 19 (2013) 2070–2083.
- [30] P. Sanphui, N.R. Goud, U.B. Rao Khandavilli, A. Nangia, Fast dissolving curcumin cocrystals, *Cryst. Growth Des.* 11 (2011) 4135–4145, <https://doi.org/10.1021/cg200704s>.
- [31] K. Kho, D. Nugroho, A.K. Sugih, Preparation and characterization of highly water soluble curcumin–dextrose cocrystal, *J. Pure. App. Chem. Res* 7 (2018) 140–148, <https://doi.org/10.21776/ub.jpacr.2018.007.02.401>.
- [32] W. Pang, Y. Wu, N. Xue, Y. Li, S. Du, B. He, C. Yang, J. Wang, Y. Zeng, Cocrystals of curcumin-isonicotinamide and curcumin-gallic acid: does the weak forces in cocrystals effect on binding profiles with BSA and cell cytotoxicity? *Eur. J. Pharm. Biopharm.* 140 (2019) 78–90, <https://doi.org/10.1016/j.ejpb.2019.05.005>.
- [33] H. Su, H. He, Y. Tian, N. Zhao, F. Sun, X. Zhang, Q. Jiang, G. Zhu, Syntheses and characterizations of two curcumin-based cocrystals, *Inorg. Chem. Commun.* 55 (2015) 92–95, <https://doi.org/10.1016/j.inoche.2015.03.027>.
- [34] N. Rath, A. Paradkar, V.G. Gaikar, Polymorphs of curcumin and its cocrystals with cinnamic acid, *J. Pharm. Sci.* 108 (2019) 2505–2516, <https://doi.org/10.1016/j.xphs.2019.03.014>.
- [35] I. Sathisaran, S.V. Dalvi, Crystal engineering of curcumin with salicylic acid and hydroxyquinol as cofomers, *Cryst. Growth Des.* 17 (2017) 3974–3988, <https://doi.org/10.1021/acs.cgd.7b00599>.
- [36] N.R. Goud, K. Suresh, P. Sanphui, A. Nangia, Fast dissolving eutectic compositions of curcumin, *Int. J. Pharm.* 439 (2012) 63–72, <https://doi.org/10.1016/j.ijpharm.2012.09.045>.
- [37] I. Sathisaran, J.M. Skieneh, S. Rohani, S.V. Dalvi, Curcumin eutectics with enhanced dissolution rates: binary phase diagrams, characterization, and dissolution studies, *J. Chem. Eng. Data* 63 (2018) 3652–3671, <https://doi.org/10.1021/acs.jced.7b01105>.
- [38] M.K.C. Mannava, K. Suresh, M.K. Bommaka, D.B. Konga, A. Nangia, Curcumin-artemisinin co-amorphous solid: xenograft model preclinical study, *Pharmaceutics* 10 (2018) 1–16, <https://doi.org/10.3390/pharmaceutics10010007>.
- [39] W. Pang, J. Lv, S. Du, J. Wang, J. Wang, Y. Zeng, Preparation of curcumin-piperazine co-amorphous phase and fluorescence spectroscopic and density functional theory simulation studies on the interaction with bovine serum albumin, *Mol. Pharm.* 14 (2017) 3013–3024, <https://doi.org/10.1021/acs.molpharmaceut.7b00217>.
- [40] J.M. Skieneh, I. Sathisaran, S.V. Dalvi, S. Rohani, Co-amorphous form of curcumin-folic acid dihydrate with increased dissolution rate, *Cryst. Growth Des.* 17 (2017) 6273–6280, <https://doi.org/10.1021/acs.cgd.7b00947>.
- [41] K. Suresh, M.K.C. Mannava, A. Nangia, A novel curcumin-artemisinin co-amorphous solid: physical properties and pharmacokinetic profile, *RSC Adv.* 4 (2014) 58357–58361, <https://doi.org/10.1039/C4RA11935E>.
- [42] P.G. Karade, N.R. Jadhav, Colon targeted curcumin microspheres laden with ascorbic acid for bioavailability enhancement, *J. Microencapsul.* 35 (2018) 372–380, <https://doi.org/10.1080/02652048.2018.1501111>.
- [43] S.J. Devaki, R.L. Raveendran, Vitamin C: Sources, Functions, Sensing and Analysis, *Intech*, 2017, pp. 1–20, <https://doi.org/10.5772/intechopen.70162>.
- [44] K. Iqbal, A. Khan, M.M. Khattak, Biological significance of ascorbic acid (vitamin C) in human health - a review, *Pak. J. Nutr* 3 (2004) 5–13, <https://doi.org/10.3923/pjn.2004.5.13>.
- [45] G. Grosso, R. Bei, A. Mistretta, S. Marventano, G. Calabrese, L. Masuelli, M. G. Giganti, A. Modesti, F. Galvano, D. Gazzolo, Effects of vitamin C on health: a review of evidence, *Front. Biosci.* 18 (2013) 1–16, <https://doi.org/10.2741/4160>.
- [46] S. Kumar, A. Nanda, Pharmaceutical cocrystals: an overview, *Indian J. Pharm. Sci* 79 (2017) 858–871, <https://doi.org/10.4172/pharmaceutical-sciences.1000302>.
- [47] N.H. Salunkhe, N.R. Jadhav, H.N. More, A.D. Jadhav, Screening of drug-sericin solid dispersions for improved solubility and dissolution, *Int. J. Biol. Macromol.* 107 (2018) 1683–1691, <https://doi.org/10.1016/j.ijbiomac.2017.10.035>.
- [48] S.P. Parimita, Y.V. Ramshankar, S. Suresh, T.N. Guru Row, Redetermination of curcumin:(1E,4Z,6E)-5-hydr-oxy-1,7-bis-(4-hydr-oxy-3-methoxy-phen-yl)hepta-

- 1,4,6-trien-3-one, Acta Cryst.E 63 (2007), <https://doi.org/10.1107/S160053680700222X>, 0860-0862.
- [49] C.J. McMonagle, M.R. Probert, Reducing the background of ultra-low-temperature X-ray diffraction data through new methods and advanced materials, J. Appl. Crystallogr. 52 (2019) 445–450.
- [50] M.M. Ribas, G.P.S. Muller, A.M. Siebel, M. Lanza, J.V. Oliveira, Curcumin-nicotinamide cocrystallization with supercritical solvent (CSS): synthesis, characterization and in vivo antinociceptive and antiinflammatory activities, Ind. Crops Prod 139 (2019) 111537, <https://doi.org/10.1016/j.indcrop.2019.111537>.